# Formation Control of Multi-agent Systems with Location Uncertainty

Markus Fröhle, Themistoklis Charalambous, Henk Wymeersch, Siwei Zhang,
Armin Dammann

**Abstract** In this chapter the impact of realistic communication channels and uncertain location information on formation control of multi-agent systems aiming to achieve a common task is highlighted. First, the work is motivated by elucidating the need to incorporate realistic communication models as well as the need to model the agents location uncertainty. Second, it is discussed how control can be utilised to reduce the agents positioning error in cooperative systems to achieve a higher level goal, such as steering a group of agents towards a destination. Third, the impact of location uncertainty on channel gain prediction is addressed for formation control. Finally, conclusions and an outlook on future directions for controlled multi-agent systems is provided.

Markus Fröhle
Chalmers University of Technology, Gothenburg, Sweden, e-mail: frohle@chalmers.se

Themistoklis Charalambous
Chalmers University of Technology, Gothenburg, Sweden, e-mail: thecha@chalmers.se

Henk Wymeersch
Chalmers University of Technology, Gothenburg, Sweden, e-mail: henkw@chalmers.se

Siwei Zhang
German Aerospace Center (DLR), Wessling, Germany, e-mail: siwei.zhang@dlr.de

Armin Dammann
German Aerospace Center (DLR), Wessling, Germany, e-mail: Armin.Dammann@dlr.de

# 1 Introduction

Increasingly sophisticated algorithms implemented on autonomous agents/robots with massive computational capabilities have enabled solving complex tasks in uncertain environments, such as mapping of disasters and search-and-rescue operations. For agents to explore and interact with the environment, it is important that they have a coherent view of this environment and their positions within it (see, for example, [1, 2] and references therein). Such situational awareness is typically achieved through simultaneous localisation and mapping (SLAM) [3] and localisation using heterogeneous sensor fusion [4]. While research on situational awareness has traditionally focused on improving the localisation accuracy, the focus has now shifted to localisation methods that have knowledge of computational complexity limitations of the agents, energy and communication constraints as well as the agent's higher-level task [5, 6]; for instance, a higher-level task may be the navigation of the robot in the environment from its current position to its final position. This chapter considers the problem of how position uncertainty in multi-agent systems affects control and communication, and how positioning can be improved taking into account the underlying limitations of such systems.

To support positioning, a robot is typically equipped with a plurality of sensors providing position information. Since the usage of these sensors consumes energy, selection of which sensor(s) to use when is important. This *sensor selection* problem refers to the agent choosing a subset out of all available sensors, in order to optimise an objective (e.g., trace or determinant of the state estimation error covariance [7, 8], an expected utility defined by Bayes risk [9], or a measure of information such as conditional entropy [10]). The objective can be optimized (i) over a single time-step [7–9, 11] or (ii) over a prediction window [10, 12–14]. In the first class of approaches, the problems made temporally separable, leading to efficient solutions [7–9, 11]. In the more general second class of approaches, the problems are temporally inherently inseparable, leading to exponential complexity in the prediction horizon. This complexity is reduced through appropriate techniques [10, 12–14]. These techniques generally focus on minimising a function of the state error covariance, which is not always relevant for battery-constrained devices. For such devices, minimising energy consumption is more meaningful, while ensuring a certain positioning quality.

While sensor selection can be performed on a per-agent basis, agents can also *cooperate* to solve tasks by combining agents with heterogeneous sensors, such as formation control [15]. Accomplishing such tasks relies on accurate and fresh location information. Existing approaches [16–20] assume perfect position information, which may not be available in reality. The limited range of the anchor signals can be countered by cooperation among agents, in order to determine the position of all agents. Cooperative positioning based on belief propagation and message passing algorithms was presented in [21]. This was extended by [22], accounting for the overhead and cost related to accessing the radio channel by a time-division multiple access protocol using an orthogonal-frequency division multiplexing (OFDM) signal. The Cramér-Rao bound (CRB) for cooperative positioning accuracy intro-

duced in [23] provides the fundamental limit of this approach. Therefore, formation control should account for localization errors [24], which can be improved through active information seeking [25, 26].

Finally, when performing a task, agents need to know their own absolute location, both for control and to maintain connectivity with each other over the wireless channel. Connectivity can be improved through *prediction of channel gains* [27]. The channel comprises three components: deterministic path-loss, shadowing, and small-scale fading [28]. The latter two components are generally modeled as random variables. For typical wave-lengths, small-scale fading decorrelates over a few centimetres, whereas shadowing decorrelates over 50–100 m outdoors [28] and 1–5 m indoors [29, 30], based on standard shadowing correlation models [31, 32]. For a multi-agent system, [33] modeled shadowing through a spatial loss field. Channel prediction was studied in [5], which proposed a Gaussian Process (GP) framework, and [34], which considered the impact of the channel parameters on the prediction variance. An assumption in [5, 33, 34] was the availability of perfect location information. This was partially addressed in [35], which extended [34] to determine the impact of localisation errors on channel prediction. Location uncertainty at the receiver but not the transmitter side was explicitly accounted for in [36].

This chapter covers recent progress in the above-mentioned areas: sensor selection, cooperation, and channel prediction. In particular, the rest of the chapter is organised as follows. We first describe several fundamental concepts in the areas on communication, control, and localisation in Section 2. We then consider the interaction between control and localisation in Section 3. In particular, Section 3.1 considers the sensor selection problem, where the aim is to find a path to a goal with minimum sensing cost, while maintaining a certain localisation quality. Section 3.2 focuses on a cooperative scenario, where again a goal must be achieved, but agents cooperate to maintain a certain localisation quality, rather than relying on a variety of sensors. In Section 4, the problem of channel prediction under location uncertainty will be tackled. These problems highlight the need to maintain good position quality in Multi-Agent Systems (MAS).

### *Link to MULTI-POS*

The work described in this chapter was carried out during 2013–2015 in the context of the FP7 project MULTI-POS, a Marie Curie International Training Network on multi-technology positioning. In particular, the work dealt with so-called cognitive methods for positioning and communication, where cognition refers to the property of the positioning and communication sub-systems to not be considered as separate, but rather as closely interacting entities. Part of this work was performed in collaboration with the German Aerospace Center, and is based on the published research papers [37–39].

## 2 Localisation for Communication and Control

This section briefly highlights the use of localisation for communication and control of MAS. We first describe a standard communication model in Section 2.1, followed by a generic optimal control problem in Section 2.2, and a metric to assess localisation algorithms in Section 2.3.

### *2.1 Inter-agent Communication*

In MAS, the communication between agents occurs over the wireless medium. The channel power between a transmitter (TX) and a receiver (RX), with locations $\mathbf{p}_{\text{TX}} \in \mathbb{R}^D$ and $\mathbf{p}_{\text{RX}} \in \mathbb{R}^D$, respectively, where $D$ is the dimensionality of the space, can be modelled as a spatially correlated random process. Assuming communication averages out small-scale fading, either in time (over a time window) or frequency (average power over a large frequency band), the received signal power in dBm can be expressed as [28]

$$P_{\text{RX}}(\mathbf{p}_{\text{TX}}, \mathbf{p}_{\text{RX}}) = P_{\text{TX}} + L_0 - 10\,\eta\,\log_{10}\frac{\|\mathbf{p}_{\text{TX}} - \mathbf{p}_{\text{RX}}\|}{d_0} + \Psi(\mathbf{p}_{\text{TX}}, \mathbf{p}_{\text{RX}}), \quad (1)$$

where the transmitted power is $P_{\text{TX}}$, $L_0$ comprises antenna and propagation gains, $d_0$ is a reference distance (here 1 m), $\eta$ is the path-loss exponent. Shadowing (in the dB domain) is modelled as a zero-mean Gaussian random process with a given spatial correlation [31, 40] and exhibiting channel reciprocity (i.e., $\Psi(\mathbf{p}_{\text{TX}}, \mathbf{p}_{\text{RX}}) = \Psi(\mathbf{p}_{\text{RX}}, \mathbf{p}_{\text{TX}})$). Provided there are no significant changes in the environment, the received power is thus largely predictable and dependent on the absolute positions of the TX and RX. Hence, in order to predict the power, the locations of the TX and RX should be known.

### *2.2 Multi-agent Control*

Control of MAS usually involves the design of optimal control strategies that should be distributed, relying on local information only. These optimal control strategies emerge from having the interconnected agents to optimise an objective function $f : \mathscr{X} \times \mathscr{U} \mapsto \mathbb{R}$, i.e.,

$$\begin{aligned} \underset{\mathbf{u} \in \mathscr{U}}{\text{minimize}} \quad & f(\mathbf{x}, \mathbf{u}) \\ \text{subject to} \quad & \dot{\mathbf{x}} = h(\mathbf{x}_0, \mathbf{u}, t), \end{aligned} \quad (2)$$

where $\mathbf{x} \in \mathscr{X}$ comprises the state of the agents (e.g., position and velocity of multiple agents over a certain time window), $\mathbf{x}_0$ represents the initial state, $\mathbf{u}$ denotes the

control input (e.g., an acceleration), belonging to some fixed set $\mathscr{U}$, and $h(\cdot)$ represents the dynamics. From the above formulation, it is clear that solving the problem in a decentralised fashion, where agents find the optimal solution without a central coordinator, information exchange between the interconnected agents regarding their state (including the position) is necessary.

## 2.3 Bounding Uncertainty of Estimators: The Cramér-Rao Bound

The Cramér-Rao Bound (CRB) is a lower bound on the estimation error variance of any unbiased estimator [23]. Due to its computational simplicity, the CRB is an attractive tool for system verification [22] and adaptive algorithm design [41]. The CRB is expressed as

$$\mathbb{E}\left[\|\hat{\mathbf{x}}^{(k)} - \mathbf{x}^{(k)}\|^2\right] \geq \text{CRB}[\mathbf{x}^{(k)}] = \text{tr}\left((\mathbf{F}_{\mathbf{x}}^{(k)})^{-1}\right), \qquad (3)$$

where $\hat{\mathbf{x}}^{(k)}$ is the estimate of $\mathbf{x}^{(k)}$ and $\mathbf{F}_{\mathbf{x}}^{(k)}$ is the so-called Fisher information matrix (FIM) with respect to $\mathbf{x}$ at time-step $k$. The FIM is defined as

$$\mathbf{F}_{\mathbf{x}}^{(k)} = -\mathbb{E}_{\mathbf{y}^{(k)}|\mathbf{x}^{(k)}}\left[\nabla_{\mathbf{x}}^{\text{T}}\nabla_{\mathbf{x}}\log p(\mathbf{y}^{(k)}|\mathbf{x}^{(k)})\right], \qquad (4)$$

where $\mathbf{y}^{(k)}$ is the measurement associated with state $\mathbf{x}^{(k)}$.

## 3 Impact of Location Uncertainty on Mission Goals

In this section, we will focus on the connection between localisation and control of agents towards a goal. Two different problems will be discussed: the first one deals with selecting paths that minimize a long-term cost, while the second one deals with progressively moving towards a goal, while also optimizing positioning quality. Both of these problems will rely on the concepts previously introduced: optimization for the control actions, and FIM for the positioning quality.

### 3.1 Limiting Location Uncertainty

#### 3.1.1 Problem Formulation

Exemplified in Fig. 1, a mobile agent with an estimated start position $\mathbf{p}_0$ aims to reach a goal position $\mathbf{p}_{\text{goal}} \in \mathbb{R}^2$ in discrete time steps. The agent is equipped with $M$ sensors providing location information, with the use of sensor $m$ having a cost (e.g., power consumption) $c_m \geq 0$. The agent can use $J \geq 1$ different paths towards
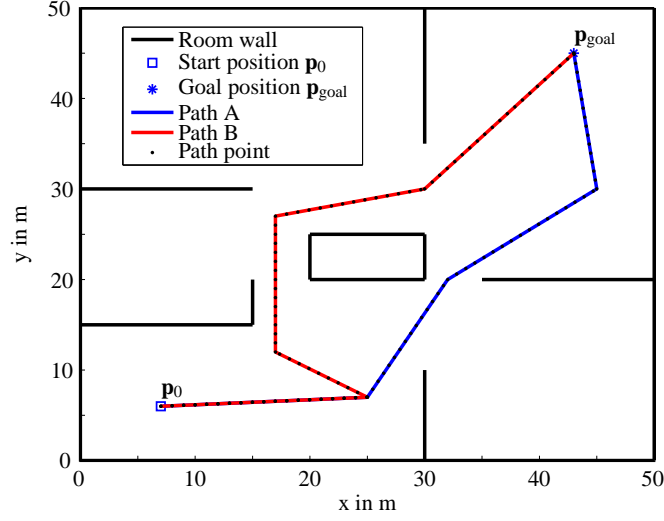
**Fig. 1** A scenario with two paths A and B from a start position $\mathbf{p}_0 = [7, 6]^{\mathrm{T}}$ to a goal position $\mathbf{p}_{\mathrm{goal}} = [43, 45]^{\mathrm{T}}$. The objective of the agent is to determine which path has the lowest cost, while ensuring a certain positioning quality.

the goal position, two of which are shown in Fig. 1. At each time and along each possible path, the agent can use at most one sensor. Each path has a certain inherent cost associated with its length (agent movement cost). The goal of the agent is to find the least expensive path to the goal, while providing a certain quality of position information.

We will consider the agent's position as its state, with the initial state $\mathbf{x}^{(0)}$ modeled as a Gaussian random variable $\mathbf{x}^{(0)} \sim \mathcal{N}(\boldsymbol{\mu}^{(0)}, \mathbf{P}^{(0)})$. The goal position $\mathbf{p}_{\mathrm{goal}}$ is known exactly, as is the floor plan of the environment and the quality of each sensor within the environment. We will focus on one of the $J$ paths, which comprises $N_j + 1$ positions, $\mathbf{p}_j^{(0)}, \mathbf{p}_j^{(1)}, \dots, \mathbf{p}_j^{(N_j)}$, where $\mathbf{p}_j^{(0)} = \boldsymbol{\mu}^{(0)}$ and $\mathbf{p}_j^{(N_j)} = \mathbf{p}_{\mathrm{goal}}$. When the agent moves along the path, its state statistics can be modeled with a process model

$$\mathbf{x}^{(k)} = \mathbf{A}^{(k-1)}\mathbf{x}^{(k-1)} + \mathbf{B}^{(k-1)}\mathbf{u}^{(k-1)} + \mathbf{n}^{(k-1)}, \tag{5}$$

where $\mathbf{u}^{(k)}$ is the control signal at time $k$, $\mathbf{A}^{(k-1)}$ and $\mathbf{B}^{(k-1)}$ are known matrices, and $\mathbf{n}^{(k-1)} \overset{\text{i.i.d.}}{\sim} \mathcal{N}(\mathbf{0}, \mathbf{Q})$ is Gaussian process noise with error covariance matrix $\mathbf{Q}$; and a measurement model of sensor $m$:

$$\mathbf{y}_m^{(k)} = \mathbf{H}_m^{(k)}\mathbf{x}^{(k)} + \mathbf{v}_m^{(k)}, \tag{6}$$

where $\mathbf{H}_m^{(k)}$ is a known matrix and $\mathbf{v}_m^{(k)} \overset{\text{i.i.d.}}{\sim} \mathcal{N}(0, \mathbf{R}_m^{(k)})$ is the measurement noise[1] associated with sensor $m$ when used in location $\mathbf{x}^{(k)}$. This linear measurement model can be motivated from a loose coupling view, where the measurement corresponds to a position estimate, as opposed to range estimates. The linear process and measurement models enable us to use the Kalman filter [43].

The agent now performs the following two steps, before proceeding to the goal.

1. For each path, the agent predicts a required control sequence $\mathbf{u}^{(0:N-1)}$, based on $\mathbf{p}^{(k)}$;
2. For a given path and a given sequence of selected sensing systems, the agent can compute (i) the expected accuracy of its predicted position using a Kalman filter and (ii) the associated cost.

The expected accuracy is determined by the FIM, introduced in Section 2.3. In particular, when the agent had a FIM $\boldsymbol{F}^{(k-1)}$ at time $k-1$ and activates sensor $m$, the FIM at time $k$ will be

$$\mathbf{F}^{(k)} = \mathbf{H}_m^{(k)\mathrm{T}} \left(\mathbf{R}_m^{(k)}\right)^{-1} \mathbf{H}_m^{(k)} + \mathbf{Q}^{-1} - \mathbf{Q}^{-1} \mathbf{A}^{(k-1)} \tag{7}$$

$$\times \left(\mathbf{F}^{(k-1)} + \left(\mathbf{A}^{(k-1)}\right)^{\mathrm{T}} \mathbf{Q}^{-1} \mathbf{A}^{(k-1)}\right)^{-1} \left(\mathbf{A}^{(k-1)}\right)^{\mathrm{T}} \mathbf{Q}^{-1},$$

Based on this information, the agent can determine the expected cost of any of the $J$ paths, and then select the least expensive path.

### 3.1.2 Optimisation Formulation

We can now cast the sensor selection problem in a standard form.

$$\underset{\mathbf{D}}{\text{minimize}} \qquad \mathbf{c}^{\mathrm{T}} \mathbf{D} \mathbf{1} \tag{8a}$$

$$\text{subject to} \qquad \mathbf{D}^{\mathrm{T}} \mathbf{1} = \mathbf{1} \tag{8b}$$

$$\mathbf{D} \in \{0,1\}^{M \times N} \tag{8c}$$

$$\mathrm{tr}\left(\left(\mathbf{F}^{(k)}\right)^{-1}\right) \leq \Delta^2, \ k \in \{1,2,\ldots,N\}, \tag{8d}$$

where $\mathbf{c} = [c_1, c_2, \ldots, c_M]^{\mathrm{T}}$, $\mathbf{1}$ is a column vector containing all ones, $\mathbf{F}^{(k)}$ is the FIM from Section 2.3 and $\mathbf{D}$ denotes the optimisation variable:

$$\mathbf{D} = \begin{bmatrix} d_1^{(1)} & \cdots & d_1^{(N)} \\ \vdots & \ddots & \vdots \\ d_M^{(1)} & \cdots & d_M^{(N)} \end{bmatrix}, \tag{9}$$

---

[1] Note that not using any sensor can be modeled by having a virtual sensor with very large covariance.

where $d_m^{(k)} = 1$ means that the $m$-th sensor system is used in the $k$-th time step; (8b) ensures that only one out of $M$ measurement systems is used at any time; (8d) ensures the trace of the inverse of the posterior FIM to stay below a specific threshold ($\Delta^2$, in m$^2$). This makes sure that that the expected[2] root mean square position error (RMSE) does not exceed $\Delta$. From (7), it is readily verified that $\mathbf{F}^{(k)}$ in (8d) can be expressed as a linear function of $\mathbf{D}$.

The problem (8) is combinatorial in nature, rendering its solution intractable as the time horizon $N$ increases. Rather than solving (8) directly, lower and upper bounds on the cost per path can be obtained through semi-definite programming (SDP), which involves relaxing the integer constraint on $\mathbf{D}$ and dynamic programming (DP), respectively. In the DP approach, we discretize the positioning quality and build up a hidden Markov model with the selected measurement systems as input. This allows us to run the Viterbi algorithm and efficiently compute the cost of any combination of measurement system selections. Additional details can be found in [38].

### 3.1.3 Performance Evaluation

We consider a scenario, detailed in [38]. In brief, the scenario is in the environment of Fig. 1, and uses a geometric path planner to generate 196 paths. We considered $M = 4$ sensor: Sensor 1 corresponds to no sensing, with $\mathbf{R}_1^{(k)} = 10^6 \, \mathbb{I}$; Sensor 2 corresponds to a GPS-like sensor which is better near the windows, but poor inside the environment; Sensor 3 is an RFID-like sensor with tags placed near the corners. Sensor 4 is an ultra-wideband-like (UWB) sensor with four reference nodes in the corners. Such a system would exhibit high sensor measurement quality in the middle of the environment, but not near the corners. We assign costs as follows: $c_1 = 1$ comprising the cost of movement, $c_2 = 3$, $c_4 = 2$, $c_4 = 4$. The DP implementation had 10 states, while the SDP implementation used the software package CVX [44]. As benchmarks, we have also implemented a greedy approach, selecting at each time step the cheapest sensor that can ensure (8d) is satisfied.

The path cost with the three different methods is evaluated for different process noise levels $\sigma_Q^2 \in \{0.01, 0.1, 0.2\}$, shown in Fig. 2, where $\mathbf{Q} = \sigma_Q^2 \, \mathbb{I}$. Paths are sorted by length. We note that when $\sigma_Q^2$ is low (top and middle plot of Fig. 2), there is a large gap between the solution using the greedy method compared to using the DP method. Hence, for low $\sigma_Q^2$ there is a clear benefit in using DP considering a long horizon. For large values of $\sigma_Q^2$, the sensors must be used more frequently to maintain acceptable positioning quality. Hence, the greedy and DP method exhibit similar performance. Furthermore, the SDP method leads to costs close to the trivial lower bound (where the cheapest sensor is used all the time). This is because the SDP method can allow for fractional sensor usage, always exactly meeting the RMSE constraint.

---

[2] Note that we only determine a path with lowest *expected* cost, under the assumption that the agent measures in the positions $\mathbf{p}_k$.
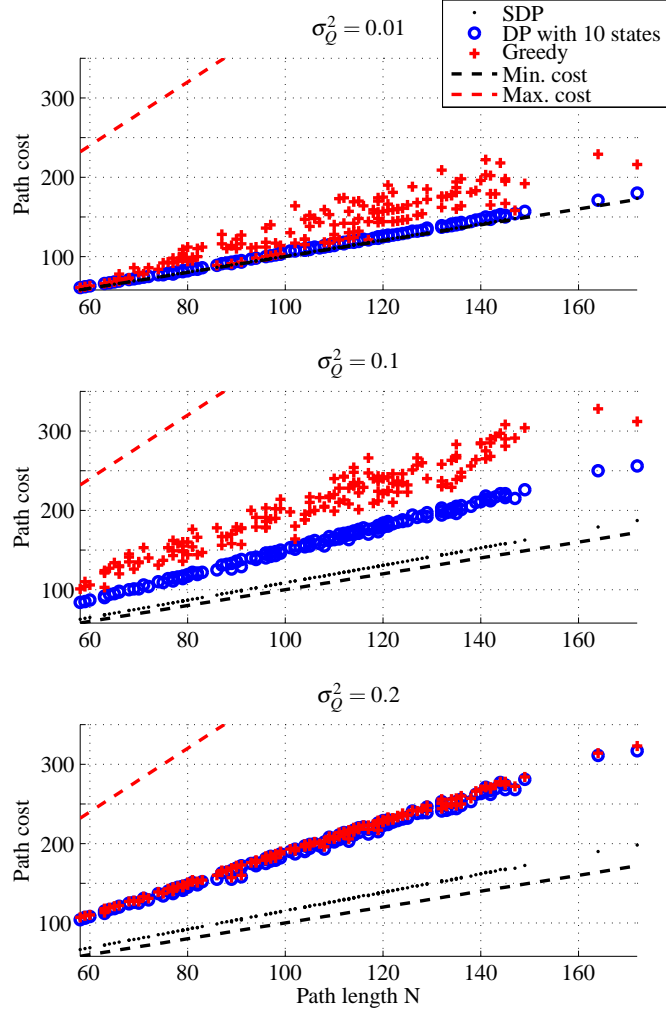
**Fig. 2** Path costs for the different paths sorted by path length. Top to bottom plot correspond to different values of the process noise variance $\sigma_Q^2 \in \{0.01, 0.1, 0.2\}$. The minimum and the maximum path costs are obtained by using the sensor with lowest and highest cost along the whole path. The lower bound (SDP) and upper bound (DP) are compared to the greedy solution.

## 3.2 Location-Aware Formation Control

The ideas from the previous section were mainly limited by the high complexity. Here, we will not consider control over a time horizon, but rather a greedy framework. This allows us to address a richer set of problems. As before, we will have a goal, but now consider multiple cooperating agents that help each other in localising as they move to the goal .

### 3.2.1 Problem Formulation

We consider a swarm of $M$ agents that want to move towards a goal with location $\mathbf{q} \in \mathbb{R}^2$, supported by anchors / base stations. We thus aim to find (global) control actions $\mathbf{u}^{(k)}$ at time $k$ moving the agents according to

$$\mathbf{p}^{(k)} = \mathbf{p}^{(k-1)} + \mathbf{u}^{(k)} + \boldsymbol{\varepsilon}^{(k)}, \tag{10}$$

where $\boldsymbol{\varepsilon}^{(k)} \sim \mathcal{N}(\mathbf{0}, \mathbf{Q})$ is the global transition noise with diagonal covariance matrix $\mathbf{Q}$. Under perfect location information this can be done by solving the optimization problem

$$\text{Problem } \mathscr{P}_\alpha: \quad \underset{\mathbf{u}_\alpha^{(k)}}{\text{minimize}} \ \|\mathbf{p}^{(k)} - \mathbf{1}_{M \times 1} \otimes \mathbf{q}\| \tag{11}$$

$$\text{subject to } \mathbf{u}_\alpha^{(k)} \in \mathscr{U}_\alpha.$$

where $\mathscr{U}_\alpha$ is a set representing all valid control signals. We will consider $\mathscr{U}_\alpha = \{\mathbf{u} \in \mathbb{R}^{2M} | \ \|\mathbf{u}\| = \mu_\alpha\}$. A goal approaching command can thus be by moving along the gradient of the objective:

$$\mathbf{u}_\alpha^{(k)} = -\mu_\alpha \frac{\mathbf{p}^{(k-1)} - \mathbf{1}_{M \times 1} \otimes \mathbf{q}}{\|\mathbf{p}^{(k-1)} - \mathbf{1}_{M \times 1} \otimes \mathbf{q}\|}. \tag{12}$$

In case the position is not known, we can replace $\mathbf{p}^{(k-1)}$ by an estimate $\hat{\mathbf{p}}^{(k-1)}$.

The problem with the above approach is that in general $\hat{\mathbf{p}}^{(k)}$ will deviate more and more from $\mathbf{p}^{(k)}$ as time $k$ progresses. To ensure that all agents stay localised, we solve the following problem

$$\text{Problem } \mathscr{P}_\beta: \quad \underset{\mathbf{u}_\beta^{(k)}}{\text{minimize}} \ \mathbb{E}\left[\|\hat{\mathbf{p}}^{(k)} - \mathbf{p}^{(k)}\|\right] \tag{13}$$

$$\text{subject to } \mathbf{u}_\beta^{(k)} \in \mathscr{U}_\beta,$$

where $\mathscr{U}_\beta = \{\mathbf{u} \in \mathbb{R}^{2M} | \ \|\mathbf{u}\| = \mu_\beta\}$ and the expectation should be interpreted as being over $\hat{\mathbf{p}}^{(k)}$.

Our goal is thus to design a swarm formation controller for joint goal-approaching and location information seeking. An example of the described swarm system is illustrated in Fig. 3, where a swarm of three agents moves from region $A$ to region $B$. Three base stations are located at each region. The white solid lines in the figure illustrate the radio connections between nodes for communications and ranging.
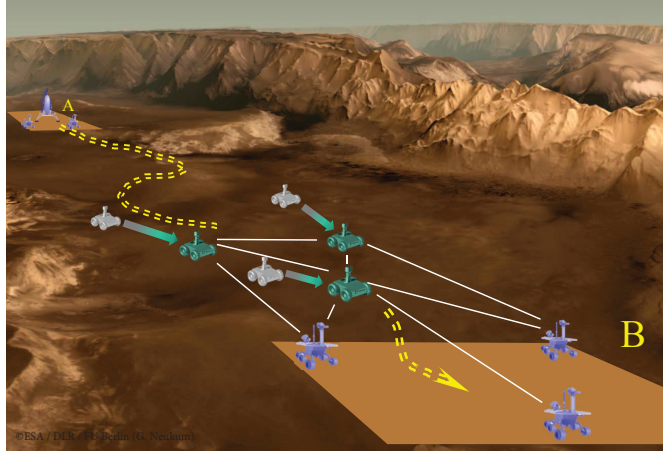
**Fig. 3** A swarm navigation system on Mars (not in real scale): three agents move from region *A* to region *B*. Three base stations are located at each region. The white solid lines illustrate the radio connections between nodes for communications and ranging.

### 3.2.2 Optimisation Formulation

We will consider an alternating optimisation approach, where the swarm alternately solves the problems $\mathscr{P}_\alpha$ and $\mathscr{P}_\beta$. Since we already provided an expression to solve $\mathscr{P}_\alpha$, we will focus on $\mathscr{P}_\beta$ and drop the time index. The problem can be expressed in terms of the Fisher Information Matrix (FIM):

$$\underset{\mathbf{u}_\beta \in \mathscr{U}_\beta}{\text{minimize}} \quad \text{tr}\left(\mathbf{F}_\mathbf{p}^{-1}\right). \tag{14}$$

The specific form of the FIM depends on the scenario at hand, the type of measurements, whether a priori information is available, etc. Considering a non-Bayesian setting, $\mathbf{F}_\mathbf{p}$ depends on the unknown value $\mathbf{p}$, which should be interpreted as the position after implementing the control (i.e., $\mathbf{p}^{(k)}$ in (10)). The gradient $\mathbf{c} \in \mathbb{R}^{2M}$ of the objective function is

$$\mathbf{c} = \left[\mathbf{c}_1^\mathsf{T}, \ldots, \mathbf{c}_u^\mathsf{T}, \ldots, \mathbf{c}_M^\mathsf{T}\right]^\mathsf{T} = \nabla_\mathbf{p} \text{tr}\left(\mathbf{F}_\mathbf{p}^{-1}\right), \tag{15}$$

where $\mathbf{c}_u \in \mathbb{R}^2$ is the gradient component of AG $u$ [39]. The steepest descent gradient controller solving $\mathscr{P}_\beta$ with a step size $\mu_\beta$ can be expressed as

$$\mathbf{u}_\beta = -\mu_\beta \frac{\mathbf{c}}{\|\mathbf{c}\|}. \tag{16}$$

Since the true positions of the agents are unknown, the gradient $\mathbf{c}$ is evaluated in the position estimates $\hat{\mathbf{p}}$ and then utilised to generate the control command $\mathbf{u}_\beta$.

As a specific instance of this problem, and to exemplify the potential for closed-form expressions, we will consider a common measurement model, as defined in Section 2.3. We let the measurements correspond to distance estimates with neighboring agents and anchors. The statistical model for the distance estimation error between nodes $u$ and $v$ with positions $\mathbf{p}_u$ and $\mathbf{p}_u$ is a zero-mean Gaussian random variable with variance $\sigma_{u,v}^2$. The ranging variance $\sigma_{u,v}^2$ is, in general, distance dependent by the radio propagation model [22]. In this work, the analytical ranging variance model proposed in [45] is applied to capture the main features of radio-based ranging. For short distances, the ranging variance is quadratically proportional to the distance. After a certain distance, the ranging variance rapidly increases to the maximum ranging variance due to the low signal-to-noise ratio (SNR).

### 3.2.3 Performance Evaluation

Simulations are conduced to illustrate the performance of the considered formation control algorithm. As initialisation, 25 agents are uniformly deployed in an area of 10 m $\times$ 10 m at region $A$. Agents need to move to region $B$ 600 meters away, based on their position estimates. In each region three base stations are deployed. Each node is equipped with a radio transceiver with coverage range of 90 meters. There is a blind region of over 400 meters along the path where none of the base stations can be directly connected due to low SNR. The step sizes are set to $\mu_\alpha = 0.15$ m and $\mu_\beta = 0.1$ m. Agents' transition noise variance at each dimension is set to 0.01 m$^2$. Two snapshots at time step 30,000 and 31,200 are shown in Fig. 4. Agents are shown as red dots and base stations as red triangles. Two magenta curves show the radio coverage border of base stations. The grey shaded background is the averaged swarm localisation CRB, i.e. $\sqrt{\mathrm{tr}(\mathbf{F}_\mathbf{p}^{-1})/M}$, when the agent of interest (marked with a green circle) moves to that position. The agent of interest can move inside the connected dark area without jeopardising the global position accuracy. The two snapshots demonstrate a procedure of establishing a virtual bridge in order to propagate high localisation accuracy into the blind region. The swarm automatically stretches to a double-row formation along $x$ dimension to extend the locatable area. At step 30,000 the agents in the middle, e.g. the one marked with green, can only move within a limited area since they are crucial vertices to maintain rigidity of the whole network. Whereas the agents clustered in front of the swarm are more flexible to move due to the redundant links. As a consequence, the crucial agents in the middle mainly perform location information seeking and the ones in front are dominantly controlled with goal-approaching. At step 31,200, the front agents have already moved inside the coverage of the base stations at region $B$ and can propagate precise position information acquired from base stations as well. Therefore, the agents behind are released from their role of crucial vertices and can apply goal-approaching again. From the figure it can be seen that the connected dark area in which the agent of interest can move is significantly increased. With this numerical result, it can be concluded that the swarm location information seeking and goal
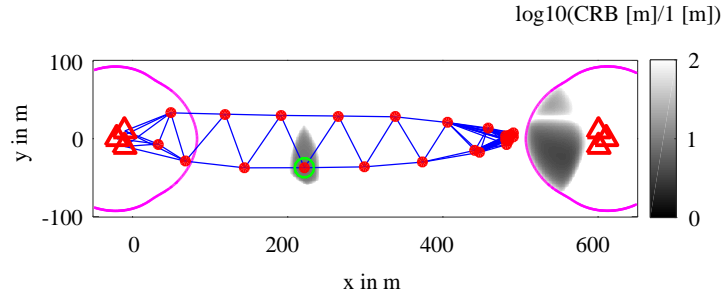
(a) step 30,000
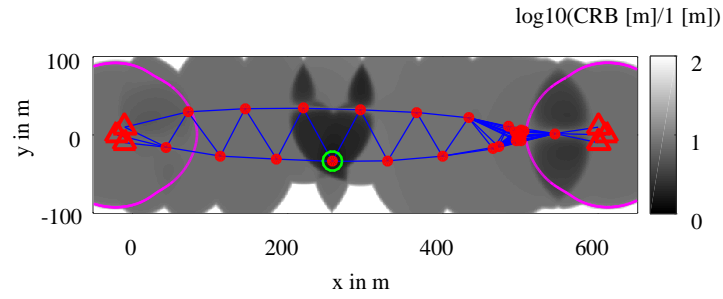


(b) step 31,200

**Fig. 4** Formation at time steps 30,000 (upper) and 31,200 (lower): agents are shown as red dots and base stations as red triangles. Two magenta curves show the radio coverage borders of base stations. The grey shaded background is the averaged swarm localisation CRB when the agent of interest (marked with a green circle) moves to that position.

approaching can be achieved with the considered formation control algorithm. The location information seeking framework can be adapted to different applications, e.g. swarm return-to-base application, where both swarm and base positions are to be estimated [47].

## 4 Impact of Location Uncertainty on Channel Gain Prediction

In this section, we step away from the control aspect and rather deal with channel modelling and prediction in the presence of location uncertainty. We will again rely on ideas introduced in Section 2.

### 4.1 Problem Formulation

A database of $N$ power measurements is available between different TX and RX locations. Each measurement is of the form $y=P_{\mathrm{RX}}(\mathbf{x})+n$, where $n \sim \mathcal{N}_n(0,\sigma_n^2)$ and the total set of measurements is denoted $\mathbf{y} = [y_1,y_2,\ldots,y_N]^{\mathrm{T}}$. The locations of both TX and RX are known statistically, through the probability density functions (pdfs) $p(\mathbf{p}_{\mathrm{TX}})$ and $p(\mathbf{p}_{\mathrm{RX}})$, which are assumed to be described by a finite number of parameters $\mathbf{s}$ (e.g., means and covariances of both agents' locations). Hence, the distributions associated with the $N$ measurements can be denoted by $\mathbf{S} = [\mathbf{s}_1^{\mathrm{T}},\mathbf{s}_2^{\mathrm{T}},\ldots,\mathbf{s}_N^{\mathrm{T}}]^{\mathrm{T}}$. For notational convenience, the positions of a TX–RX pair will be denoted by $\mathbf{x} = [\mathbf{p}_{\mathrm{TX}}^{\mathrm{T}},\mathbf{p}_{\mathrm{RX}}^{\mathrm{T}}]^{\mathrm{T}} \in \mathbb{R}^{2D}$, allowing expressions such as $P_{\mathrm{RX}}(\mathbf{x})$ and $P_{\mathrm{RX}}(\mathbf{s}) = \int P_{\mathrm{RX}}(\mathbf{x})p(\mathbf{x})\mathrm{d}\mathbf{x}$ .

The problems considered in this section are (i) learning of channel parameters; (ii) prediction of the channel at an unvisited location.

### 4.2 Channel Prediction

The Gaussian process (GP) framework of [36], called uncertain GP (uGP), is here adapted for learning and prediction of the wireless channel considering TX and RX location uncertainty. This uGP framework is contrasted to classical GP (cGP), wherein location uncertainty is ignored. The simplify the exposition, we will ignore the deterministic path loss, and consider only shadowing. The received power at uncertain location pair $\mathbf{x}$ (described by its distribution parameters $\mathbf{s}$) is modelled as a GP, denoted by

$$P_{\mathrm{RX}}(\mathbf{s}) \sim \mathscr{GP}\left(0, k(\mathbf{s},\mathbf{s}')\right), \tag{17}$$

where a suitable choice for the covariance function is

$$k(\mathbf{s},\mathbf{s}') = \iint c(\mathbf{x},\mathbf{x}')p(\mathbf{x})p(\mathbf{x}')\mathrm{d}\mathbf{x}\,\mathrm{d}\mathbf{x}', \tag{18}$$

in which $c(\mathbf{x},\mathbf{x}')$ is a covariance function under precise location information. Note that (18) reverts back to a classical GP (cGP) approach, with classical covariance functions [5], when there is no location uncertainty. In order to obtain a closed-form

expression for (18), $c(\mathbf{x}, \mathbf{x}')$ should be limited to certain specific families, e.g., a squared exponential. In that case, with $p = 2$, one can write

$$c(\mathbf{x}, \mathbf{x}') = \sigma_\Psi^2 \exp\left( -\frac{\|\mathbf{p}_{TX} - \mathbf{p}'_{TX}\|^p}{d_c^p} - \frac{\|\mathbf{p}_{RX} - \mathbf{p}'_{RX}\|^p}{d_c^p} \right), \qquad (19)$$

when $\mathbf{x} \neq \mathbf{x}'$ and $c(\mathbf{x}, \mathbf{x}) = \sigma_\Psi^2 + \sigma_{proc}^2$. The problem of learning now involves determining the parameters $\theta = [d_c, \sigma_\Psi, \sigma_{proc}]$ from the database. Once $\theta$ has been determined, the prediction problem can then be solved, by virtue of using a GP framework.
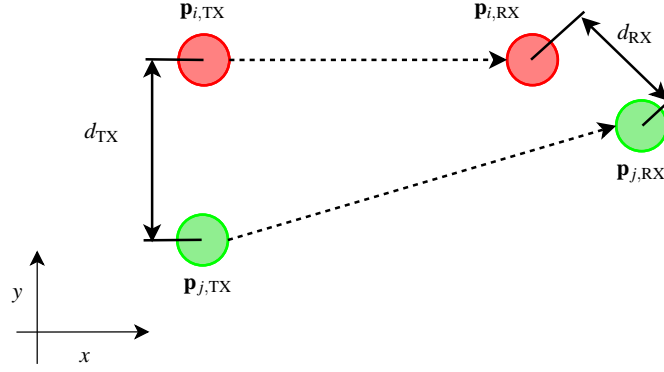


**Fig. 5** Example of two links $i$ and $j$ in $\mathbb{R}^2$. The transmitter displacement is given by $d_{TX} = \|\mathbf{p}_{i,TX} - \mathbf{p}_{j,TX}\|$ and the receiver displacement is $d_{RX} = \|\mathbf{p}_{i,RX} - \mathbf{p}_{j,RX}\|$.
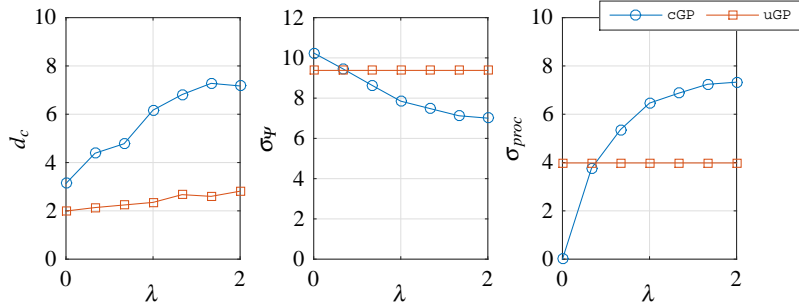


**Fig. 6** Estimated hyper parameters for cGP and uGP for different levels of location uncertainty of the training samples parametrized by the average location error standard deviation $\lambda$ in meters. Left: decorrelation distance $d_c$, middle: shadow standard deviation $\sigma_\Psi$, right: process standard deviation $\sigma_{proc}$.
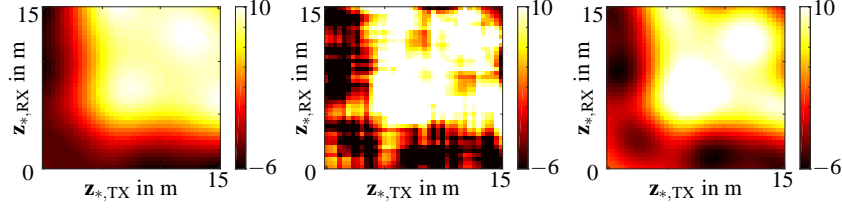
**Fig. 7** Left: expected received power $P_{RX,avg}$ for one realisation of the spatially correlated shadowing field for different expected positions $\mathbf{z}_{*,TX}$, and $\mathbf{z}_{*,RX}$ respectively. The channel is symmetric reciprocal along the diagonal ($\mathbf{z}_{*,TX} = \mathbf{z}_{*,RX}$), i.e., the field is symmetric. Middle: prediction of $P_{RX,avg}$ using cGP. Right: prediction of $P_{RX,avg}$ using uGP. Note, cGP and uGP maintain channel reciprocity in their prediction.

## 4.3 Performance Evaluation

We consider a one-dimensional zero-mean field of 15 m length: $P_{RX}(\mathbf{x}) : [0, 15] \times [0, 15] \to \mathbb{R}$. The true field is obtained from a 2-dimensional GP with (19), with parameters $p = 1$, $d_c = 3$, $\sigma_n = 0.01$, and $\sigma_\Psi = 10$. To ensure reciprocity the field is only generated for $\mathbf{p}_{TX} \geq \mathbf{p}_{RX}$ and then copying the values for $\mathbf{p}_{TX} < \mathbf{p}_{RX}$. The resolution of the field is 25 cm, corresponding to possible 40 TX and RX locations, which in total corresponds to 1600 samples. For the training set $N = 250$ samples are randomly selected out of these 1600 samples. This includes their reciprocal counterpart. They are then perturbed by location uncertainty. In accordance with [36], heterogeneous location errors have been considered with error variance $\sigma_i$. The error variance follows an exponential distribution parametrized by the average location error standard deviation $\lambda$. Assuming the agents know $\sigma_n$, the hyper-parameter vector is then given by $\theta = [d_c, \sigma_\Psi, \sigma_{proc}]^T$. The covariance function of cGP corresponds to the Gudmundson model [31]. For parameter learning, a Monte Carlo simulation is performed over 30 realisations of the shadowing field.

**Learning**

The influence of location uncertainty of the training samples (parametrised by $\lambda$) in the database on the estimation of $\theta$ for cGP (with $p = 1$) and uGP (with $p = 2$) is demonstrated in Fig. 6. For cGP, it can be observed that an increase of $\lambda$ leads to an increase of $d_c$. Furthermore, the parameter responsible for capturing input uncertainty $\sigma_{proc}$ also increases. To maintain the total signal variance the parameter $\sigma_\Psi$ needs to decrease. In contrast to this, uGP is able to properly incorporate different levels of location uncertainty with the effect that the estimated $d_c$ remains almost constant independent of the location uncertainty of the training samples. The parameter $\sigma_{proc}$ captures the mismatch between the covariance functions of the true field (where $p = 1$ in (19)) and uGP (where $p = 2$ in (19)). This mismatch is independent of the location uncertainty of the training samples $\lambda$. In the right plot of

Fig. 6, this can be observed by the estimated values of $\sigma_{\text{proc}}$. This means, since $\sigma_{\text{proc}}$ is constant over $\lambda$ so has to be $\sigma_{\Psi}$ in order to maintain the total variance (see middle panel of Fig. 6).

**Prediction**

The prediction performance is shown in Fig. 7, assuming the database had no location uncertainty (i.e., $\lambda = 0$), but the received power should be predicted at a location where a location uncertainty with standard deviation 2 meters is present. The expected received power is expressed by $P_{\text{RX,avg}}(\mathbf{s}_*) = \int P_{\text{RX}}(\mathbf{x}_*)p(\mathbf{x}_*)\mathrm{d}\mathbf{x}_*$. Here, $p(\mathbf{x}_*) = \mathcal{N}_{\mathbf{x}_*}(\mathbf{z}_*, 4\mathbf{I})$. The mean value of the random location $\mathbf{x}_*$ is composed of the TX and RX mean location by $\mathbf{z}_* = [\mathbf{z}_{*,\text{TX}}, \mathbf{z}_{*,\text{RX}}]^{\text{T}}$. The panels of Fig. 7 contain from left to right: $P_{\text{RX,avg}}$ plot for different mean transmitter and receiver locations ($\mathbf{z}_{*,\text{TX}}$ and $\mathbf{z}_{*,\text{TX}}$), predicted expected received power with cGP, and with uGP. Observe that with both methods, cGP and uGP, channel reciprocity is maintained. Furthermore, the prediction of the true expected field with uGP is much better than with cGP.

## 5 Conclusion

The foreseeable emerging applications suggest that MAS are likely to become more prevalent in the coming years. Specific instances include intelligent transportation systems, networks of unmanned aerial vehicles (e.g., drones), networks of wheel-driven robots, or even a network comprised of heterogeneous agents. All these systems rely heavily on precise location information. This chapter treated how location information can be obtained, maintained, and disseminated over a network of agents. It also revealed a close connection between communication and localisation, and described a channel prediction strategy in the presence of location uncertainty. Furthermore, the coupling between communication and control and their dependencies on localisation have been demonstrated. Significant challenges remain, both to provide accurate location information, and to operate MAS under limited, noisy or no information about the location of the agents.

## Acknowledgment

# References

1. Gunar Schirner, Deniz Erdogmus, Kaushik Chowdhury, and Taskin Padir. The Future of Human-in-the-Loop Cyber-Physical Systems. *Computer*, 46(1):36–45, 2013.
2. GJM Kruijff, M Janíček, S Keshavdas, B Larochelle, H Zender, NJJM Smets, T Mioch, MA Neerincx, JV Diggelen, F Colas, et al. Experience in System Design for Human-Robot Teaming in Urban Search and Rescue. In *Field and Service Robotics*, pages 111–125. Springer, 2014.
3. Sebastian Thrun and Yufeng Liu. Multi-robot SLAM with Sparse Extended Information Filers. In *Robotics Research*, pages 254–266. Springer, 2005.
4. Henk Wymeersch, Jaime Lien, and Moe Z Win. Cooperative Localization in Wireless Networks. *Proceedings of the IEEE*, 97(2):427–450, 2009.
5. Jonathan Fink. *Communication for teams of networked robots*. PhD thesis, Penn, University of Pennsylvania, 2011.
6. G.E. Garcia, L.S. Muppirisetty, E.M. Schiller, and H. Wymeersch. On the Trade-Off Between Accuracy and Delay in Cooperative UWB Localization: Performance Bounds and Scaling Laws. *Wireless Communications, IEEE Transactions on*, 13(8):4574–4585, Aug 2014.
7. Siddharth Joshi and Stephen Boyd. Sensor Selection via Convex Optimization. *IEEE Transactions on Signal Processing*, 57(2):451–462, 2009.
8. Manohar Shamaiah, Siddhartha Banerjee, and Haris Vikalo. Greedy Sensor Selection: Leveraging Submodularity. In *49th IEEE Conference on Decision and Control (CDC)*, pages 2572–2577. IEEE, 2010.
9. David Cohen, Douglas L Jones, and Sriram Narayanan. Expected-utility-based Sensor Selection for State Estimation. In *IEEE International Conference on Acoustics, Speech and Signal Processing (ICASSP)*, pages 2685–2688. IEEE, 2012.
10. Jason L Williams, John W Fisher, and Alan S Willsky. Approximate Dynamic Programming for Communication-Constrained Sensor Network Management. *IEEE Transactions on Signal Processing*, 55(8):4300–4311, 2007.
11. Amit S Chhetri, Darryl Morrell, and Antonia Papandreou-Suppappola. On the Use of Binary Programming for Sensor Scheduling. *IEEE Transactions on Signal Processing*, 55(6):2826–2839, 2007.
12. Xiaojing Shen and P.K. Varshney. Sensor Selection Based on Generalized Information Gain for Target Tracking in Large Sensor Networks. *IEEE Transactions on Signal Processing*, 62(2):363–375, Jan 2014.
13. Michael P Vitus, Wei Zhang, Alessandro Abate, Jianghai Hu, and Claire J Tomlin. On Efficient Sensor Scheduling for Linear Dynamical Systems. *Automatica*, 48(10):2482–2493, 2012.
14. M.F. Huber. On Multi-Step Sensor Scheduling via Convex Optimization. In *2nd International Workshop on Cognitive Information Processing (CIP)*, pages 376–381, June 2010.
15. Jeff S Shamma, editor. *Cooperative control of distributed multi-agent systems*. Wiley Online Library, 2007.
16. R. Olfati-Saber. Flocking for Multi-Agent Dynamic Systems: Algorithms and Theory. *Automatic Control, IEEE Transactions on*, 51(3):401–420, 2006.
17. Nair Maria Maia de Abreu. Old and new results on algebraic connectivity of graphs. *Linear algebra and its applications*, 423(1):53–73, 2007.
18. Yoonsoo Kim and Mehran Mesbahi. On maximizing the second smallest eigenvalue of a state-dependent graph Laplacian. *IEEE Transactions on Automatic Control*, 51(1):116–120, 2006.
19. Yanghyun Kim, Guangwei Zhu, and Jianghai Hu. Optimizing formation rigidity under connectivity constraints. In *IEEE Conference on Decision and Control (CDC)*, pages 6590–6595, 2010.
20. Michael Zavlanos, Magnus Egerstedt, and George Pappas. Graph-theoretic connectivity control of mobile robot networks. *Proceedings of the IEEE*, 99(9):1525–1540, 2011.
21. H. Wymeersch, J. Lien, and M.Z. Win. Cooperative Localization in Wireless Networks. *Proceedings of the IEEE*, 97(2):427 –450, Feb. 2009.

22. S Zhang, R Raulefs, A Dammann, and S Sand. System-Level Performance Analysis for Bayesian Cooperative Positioning: From Global to Local. In *Proceeedings of 2013 International Conference on Indoor Position and Indoor Navigation (IPIN)*, 2013.

23. Yuan Shen, H. Wymeersch, and M.Z. Win. Fundamental limits of wideband localization - part ii: Cooperative networks. *Information Theory, IEEE Transactions on*, 56(10):4981 –5000, oct. 2010.

24. Siwei Zhang and Ronald Raulefs. Multi-agent flocking with noisy anchor-free localization. In *11th International Symposium on Wireless Communications Systems (ISWCS)*, pages 927–933, 2014.

25. F. Morbidi and G. L. Mariottini. Active target tracking and cooperative localization for teams of aerial vehicles. *IEEE Trans. Control Syst. Technol.*, 21(5):1694–1707, 2013.

26. F. Meyer, H. Wymeersch, M. Fröhle, and F. Hlawatsch. Distributed estimation with information-seeking control in agent networks. *Selected Areas in Communications, IEEE Journal on*, 2015.

27. Tugay Eyceoz, Alexandra Duel-Hallen, and Hans Hallen. Deterministic channel modeling and long range prediction of fast fading mobile radio channels. *IEEE Communications Letters*, 2(9):254–256, 1998.

28. Andrea Goldsmith. *Wireless Communications*. Cambridge University Press, 2005.

29. Annika Böttcher, Peter Vary, Christian Schneider, and Reiner S Thomä. De-correlation distance of the large scale parameters in an urban macro cell scenario. In *6th European Conference on Antennas and Propagation (EUCAP)*, pages 1417–1421, 2012.

30. Niklas Jalden. *Analysis and Modelling of Joint Channel Properties from Multi-site, Multi-Antenna Radio Measurements*. PhD thesis, KTH, Signal Processing, 2010.

31. Mikael Gudmundson. Correlation model for shadow fading in mobile radio systems. *Electronics Letters*, 27(23):2145–2146, Nov 1991.

32. Zhenyu Wang, Eustace K. Tameh, and Andrew R. Nix. Joint Shadowing Process in Urban Peer-to-Peer Radio Channels. *Vehicular Technology, IEEE Transactions on*, 57(1):52–64, Jan 2008.

33. Piyush Agrawal and Neal Patwari. Correlated link shadow fading in multi-hop wireless networks. *IEEE Transactions on Wireless Communications*, 8(8):4024–4036, 2009.

34. Mehrzad Malmirchegini and Yasamin Mostofi. On the spatial predictability of communication channels. *IEEE Transactions on Wireless Communications*, 11(3):964–978, 2012.

35. Yuan Yan and Yasamin Mostofi. Impact of localization errors on wireless channel prediction in mobile robotic networks. In *IEEE Globecom, Workshop on Wireless Networking for Unmanned Autonomous Vehicles*, Dec. 2013.

36. L. Srikar Muppirisetty, Tommy Svensson, and Henk Wymeersch. Spatial Wireless Channel Prediction under Location Uncertainty. *to appear in IEEE Transactions on Wireless Communications*, 2015.

37. Markus Fröhle, Leela Srikar Muppirisetty, and Henk Wymeersch. Channel gain prediction for multi-agent networks in the presence of location uncertainty. In *IEEE International Conference on Acoustics, Speech and Signal Processing (ICASSP)*, 2016.

38. M. Fröhle, A. A. Zaidi, E. Ström, and H. Wymeersch. Multi-step sensor selection with position uncertainty constraints. In *2014 IEEE Globecom Workshops (GC Wkshps)*, pages 1439–1444, Dec 2014.

39. Siwei Zhang, Markus Fröhle, Henk Wymeersch, Armin Dammann, and Ronald Raulefs. Location-aware formation control in swarm navigation. In *IEEE Globecom Workshops*, 2015.

40. S.S. Szyszkowicz, H. Yanikomeroglu, and J.S. Thompson. On the feasibility of wireless shadowing correlation models. *Vehicular Technology, IEEE Transactions on*, 59(9):4222–4236, Nov 2010.

41. Kallol Das and Henk Wymeersch. Censoring for Bayesian Cooperative Positioning in Dense Wireless Networks. *IEEE Journal on Selected Areas in Communications*, 30(9):1835–1842, 2012.

42. Steven Michael LaValle. *Planning Algorithms*. Cambridge university press, 2006.

43. Dan Simon. *Optimal State Estimation: Kalman, H infinity, and Nonlinear Approaches*. John Wiley & Sons, 2006.

44. Michael Grant and Stephen Boyd. CVX: Matlab Software for Disciplined Convex Programming. http://cvxr.com/cvx, March 2014.
45. Siwei Zhang, Markus Fröhle, Henk Wymeersch, Armin Dammann, and Ronald Raulefs. Location-aware formation control in swarm navigation. In *IEEE Globecom Workshop*, 2015.
46. Steven M. Kay. *Fundamentals of Statistical Signal Processing: Estimation Theory*. Prentice-Hall, Inc., Upper Saddle River, NJ, USA, 1993.
47. Siwei Zhang, Ronald Raulefs, and Armin Dammann. Localization-driven formation control for swarm return-to-base applicationn. In *European Signal Processing, 2016 IEEE/EURASIP Conference on (EUSIPCO)*, 2016.